Simulation of Ultrasonic Welding of Al-Cu Dissimilar Metals for Battery Joining

Reza Abdi Behnagh*, Peyman Esmaeilzadeh, Mohsen Agha Mohammad Pour

Faculty of Mechanical Engineering, Urmia University of Technology, Iran
E-mail: esmailzadeh.peyman@gmail.com, r.abdibehnagh@uut.ac.ir, aga.mohsen@yahoo.com
*Corresponding author

Received: 16 August 2019, Revised: 20 January 2020, Accepted: 5 February 2020

Abstract: Ultrasonic welding is gaining popularity for joining of thin and dissimilar materials and foils in the fabrication of automotive Li-ion battery packs because of excellent efficiency, high production rate, high welding quality, etc. Precise control of the parameters of the welding process plays an important role in achieving good joint quality. Numerical simulation can greatly help control the main input parameters such as frequency, clamping pressure, friction coefficient, and vibration amplitude. In this present work, a three-dimensional thermo-mechanical Finite Element (FE) model is proposed using ABAQUS/EXPLICIT for the dissimilar Al to Cu weld to predict the deformation and temperature as output parameters during welding process by varying input parameters. The simulation results showed that the clamping pressure, vibration frequency and friction coefficient have a great influence on heat production during the process which was critical to determine the final quality of the welded joint. Studies also showed that increased clamping force and welding frequency led to increased deformation.

Keywords: Aluminium, Copper, Finite Element Model, Li-Ion Battery, Ultrasonic Welding

Reference: Reza Abdi Behnagh, Peyman Esmaeilzadeh, and Mohsen Agha Mohammad Pour, "Simulation of Ultrasonic Welding of Al-Cu Dissimilar Metals for Battery Joining", Int J of Advanced Design and Manufacturing Technology, Vol. 13/No. 2, 2020, pp. 23–31.

Biographical notes: Reza Abdi Behnagh is an Assistant Professor of Mechanical Engineering at the Urmia University of Technology. He received his BSc from the Amirkabir University of Technology, Iran and MSc and PhD from the University of Tehran, Iran, respectively. His current research focuses on manufacturing and materials processing. **Peyman Esmaeilzadeh** received his MSc in Mechanical Engineering from the Urmia University of Technology in 2019. His main research interests are fracture mechanics and numerical simulation. **Mohsen Agha Mohammad Pour** received his MSc in Mechanical Engineering from the Urmia University of Technology in 2019. His main research interests are fracture mechanics and numerical simulation.

1 INTRODUCTION

The growing demand for fuel efficiency, low emission, and lightweight electrical plug-in hybrid and electric vehicles (PHEV, EV) create new possibilities in the manufacturing field. These vehicles use lithium-ion battery packs as the solution to achieve the desired power. The battery pack is usually composed of a large amount of battery cells. Due to the high electrical and thermal conductivity properties of aluminium and copper, their joints are typically used in the fabrication process of the batteries. Joining thin and dissimilar materials by the traditional fusion welding processes is difficult for two reasons; (1): poor weld ability arises from the remarkable difference in chemical, mechanical, and thermal properties of the weld materials. (2): brittle intermetallic compounds are usually formed at the joint interface and results in the decrease of the strength of the fabricated joints.

Solid-state welding techniques like Friction Stir Welding (FSW), Explosion Welding and Ultrasonic Welding (USW) limit the heat generation during the process and the joints can be formed below the materials melting points. Therefore, the risk of the formation of intermetallic compounds is significantly reduced. The past researches have shown that USW uses less energy compared with other solid-state techniques in similar welds. Murr et al. [1] revealed that Al-Cu friction stir welds do not have a good quality due to weakness and failure at the weld nugget zone. Hence, USW is becoming an essential and potential method to join Al to Cu in battery makers. USW is a rapid welding technique that produces a joint within a few seconds by applying a moderate amount of clamping pressure and tangential vibration to the work piece. The process includes compression loading in the work piece normal direction, and accordingly heat generation due to friction between work piece materials. In USW, the amount of heat generation and plastic deformation determines the quality of the joint and interface microstructure which mainly depends on the appropriate selection of process parameters. The mechanism of this process is complex for bond formation; thus, many types of research have been done to clarify this. According to those findings, frictional heating, severe plastic deformation, mechanical interlocking, and local melting are the factors can lead to the formation of a solid-state bond between the metals. Among these factors, frictional heating and heat generated from plastic deformation are mostly believed for the formation of the weld. Hence, it is essential to consider the distribution of temperature, amount of heat generated, and the amount of plastic deformation during welding for a clear understanding of the process. Any change in the input parameters results in variation in the amount of energy delivered to the weld area.

Watanable et al. [2] have worked on ultrasonic welding of mild steel sheet to Al-Mg sheet and concluded that weld strength decreases with longer welding time and higher welding pressure. Shin and Leon [3] studied on the influence of welding time on interface temperature and joint strength of Al to Cu welds. They concluded that higher vibration amplitude and shorter welding time were essential to achieve good strength. In a similar work, Yang et al. [4] demonstrated that the welding time was affected by the shear strength of the AA6061-copper lap joint. It was observed that, with increasing welding time, the shear strength increases up to a specified value and then decreases further with an increase in time.

Zhao et al. [5] experimentally studied the effect of welding energy on Al–Cu ultrasonic welded joint at different ultrasonic energy levels. They observed that at lower welding energies, the joint was only bonded by micro welds at the weld interface. Hence, the joint failed at a quite low load by debonding. The joint strength increased with increase in the ultrasonic energy and reached the maximum value at 1000 J. Elangovan et al. [6] observed that welding time is the most significant input parameter which had a great impact on joint strength followed by amplitude and welding pressure during the ultrasonic welding of copper.

Moreover, Kim et al. [7] evaluated the weld ability of the materials in ultrasonic welding of thin sheets via a third-order regression model within the robust range of input parameters. A good number of studies have also been carried out on the numerical analysis of the ultrasonic welding process and some constructive results also have been obtained. Zhang et al. [8] considered the temperature field at the weld by applying different ultrasonic energies. They concluded that the softening of the materials took place to enhance the joining of materials and the peak temperature was above 500 C at the weld center. De Vries [9] also demonstrated that the temperature rises at the interface up to around 0.4 to 0.8 of the base material melting point.

Siddiq and Ghassemieh [10] investigated the effect of both volume and surface softening effects in ultrasonic welding of one sheet of aluminium on an aluminium substrate. It was observed that increasing the welding time results in increased friction between the sheets with temperature up to a certain value, and it fell down subsequently. Elangovan [11] also carried out experiments on copper sheets with dissimilar thickness. During the experiments, the thermal history of the process was recorded using a thermocouple and a thermal imager. After experimental studies, the obtained results were further validated by Finite Element Analysis (FEA). Furthermore, Jedrasiak et al. [12] developed a 3D finite element model for the ultrasonic dissimilar welding of 6111 aluminium to AZ31 magnesium and DC04 low carbon steel. The developed model had the capability of predicting the amount of

heat generation between the tool and the top sheet and between the work piece in all material combinations. Again, a FEM based model was developed by Elangovan et al. [13] for the ultrasonic welding of aluminium to copper which predicts the temperature during the process.

Chen and Zhang [14] conducted the numerical analysis on ultrasonic welding to prospect the influence of horn patterns on the mechanical properties of the joint. The results of their work showed the development of stress, plastic strain, and deformation along the compression direction caused by the high-frequency vibration of sonotrode. Konchakova et al. [15] remarked the dependencies of the numerical values of the mechanical behaviour on the interface geometries through modelling of the mechanical properties of the joint between metal to CFRP. Lee et al. [16] worked on using hybrid explicit/implicit FEM analysis to explore the frictional heat generation in ultrasonic welding, as well as predict the weld quality to join thin Li-ion battery tabs.

From the existing literature, no adequate information is available regarding the effect of process parameters on the weld responses through numerical analysis. It should also be noted that the published works only consider simple geometric configurations, which are not realistic for applications in the automotive industry. Hence, a three-dimensional thermo-mechanical model is designed for realistic geometry configuration with moderate computational cost to investigate the effect of friction, frequency and welding pressure on temperature history, and sheets deformation during ultrasonic welding of Al to Cu thin sheets. The FE simulations are conducted with ABAQUS software in explicit mode.

2 PRINCIPLES OF ULTRASONIC WELDING

Ultrasonic metal welding uses the oscillating shears generated by high-frequency ultrasonic energy to create a solid-state bond between metals [17]. This process overcomes the joining difficulties of multiple sheets of dissimilar materials by using its inherent advantages derived from the solid-state process characteristics [16]. In addition, unlike resistance welding and laser welding, the temperature in the ultrasonic welding process does not exceed the melting point of the metal work piece, eliminating undesirable compounds, phases, and metallurgical defects that commonly exist in most other fusion welds [16], [18]. Thus, among the different joining options, ultrasonic metal welding is believed to be most suitable for battery joining. At this present study, the principle of ultrasonic welding is taken from experimental work by Lee et al. [19]. Hence, the simulation results are verified using empirical data from their work. In their study on tabs-bus joining in Li-ion battery cells, pure copper and aluminium foils were joined by an AmTech Ultraweld L-20 high power welder with a maximum output power of 4 kW. At this present study, both of the top and bottom foils were 0.2 mm in thickness. Moreover, the aluminium foil was placed on the top of the copper foil. The ultrasonic vibration was applied in traverse direction with a constant amplitude of 25 μm at three different values of frequency including 40, 50, and 60 kHz. In addition, three different clamping forces including 105, 110, 120 MPa were implemented along the vertical direction. The welding simulations were carried out using a welding time of 0.05 s. Knurl and anvil patterns are assumed to be a flat face during the simulations. The friction coefficient varied from 0.3 to 0.7 to investigate the effect of friction between the foils on output parameters. (“Table 1”)

Table 1 Materials and process parameters

Tool design	Flat face
Materials	Al (tab), Cu (bar)
Work pieces thickness (mm)	0.2
Clamping Pressure (MPa)	105, 110, 120
Clamping time (s)	25e-4
Vibration amplitude (μm)	25
Vibration frequency (kHz)	40, 50, 60
Welding time (s)	15e-4, 5e-2
Clamping time (s)	25e-4

3 THERMO-MECHANICAL ANALYSIS OF ULTRASONIC WELDING

3.1. Material Model

Ultrasonic welding produces a joint by exerting ultrasonic vibration energy to the weld coupon. The process involves compression loading by applying force on the work piece normal direction and cyclic loading in the tangential direction. The result of these two movements is the generation of frictional heat and temperature rise in the joint interface. Therefore, the process is considered as a coupled thermo-mechanical problem. In this research, some of the material parameters for aluminium and copper are considered to be temperature-dependent including thermal conductivity, specific heat, thermal expansion, and yield stress, which are shown in “Fig. 1”. While the density of the materials and material properties of the horn and anvil are assumed to be temperature independent, the density of aluminium and copper are considered to be 2.7e-9 and 8.94e-9 tonmm-3, respectively. The properties of the steel used in horn and anvil are presented in “Table 2”.

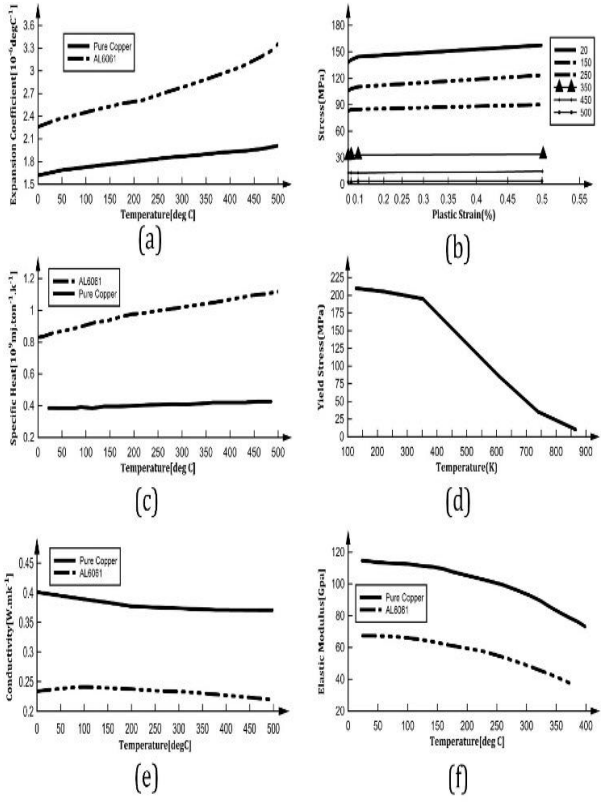

Fig. 1 Temperature-dependent thermal properties of aluminum and copper: (a): Expansion coefficient, (b): Plastic Strain, (c): specific heat, (d): Yield stress, (e): Thermal conductivity, and (f): Elastic modulus.

Table 2 Properties of the steel

Material	Steel
Density (ton mm^{-3})	7.8e-9
Specific heat (mJ $mm^{-1}°C^{-1}$)	4.4e8
Thermal conductivity (mW $mm^{-1}°C^{-1}$)	80
Elastic modulus (MPa)	2.0e5

Temperature-dependent expansion coefficient, plastic Strain, specific heat, yield stress, thermal conductivity and elastic modulus of aluminium and copper alloys are shown in "Fig. 1".

3.2. Mechanical Model

The basic constitutive equations for metal plasticity under cyclic loading were adopted from uniaxial loading. The total strain can be composed of elastic and plastic strain sensor [10]:

$$\varepsilon = \varepsilon^{el} + \varepsilon^{pl} \tag{1}$$

The elastic behaviour at any step of the simulation can be modelled as:

$$\sigma = D_{el}\boldsymbol{\varepsilon}^{el} = D_{el}(\varepsilon - \varepsilon^{pl}) \tag{2}$$

Where, D_{el} is the 4th order elasticity tensor. Then the yield function can be calculated by:

$$F = |\sigma - \alpha| - (\sigma_0 - R) = 0 \tag{3}$$

Where, α is the term related to back stress tensor, σ_0 is initial yield stress, and R represents the term related to isotropic hardening. The plastic behavior during deformation is given by:

$$d\varepsilon^{pl} = d\lambda \frac{\partial F}{\partial \sigma} \tag{4}$$

Where, $d\lambda$ is a plastic multiplier which satisfies the following Kuhn-Tucker type consistency conditions.

$$F \leq 0. d\lambda \geq 0. F, d\lambda \cong 0 \tag{5}$$

The expansion of yield surface due to isotropic hardening can be expressed as the exponential function of accumulated plastic strain [10]:

$$R = Q(1 - e^{-b\underline{\varepsilon}^{pl}}) \tag{6}$$

Where, Q and b are material constants. Q is the maximum change of yield surface due to isotropic hardening and b is the rate at which yield surface changes with accumulated equivalent plastic strain $\underline{\varepsilon}^{pl}$. For nonlinear kinematic hardening, the back-stress rate ($\boldsymbol{\alpha}$) is given by:

$$\underline{\dot{\alpha}} = C\frac{1}{\sigma_0}(\underline{\sigma} - \underline{\alpha})\dot{\underline{\varepsilon}}^{pl} - \gamma\underline{\alpha}\dot{\underline{\varepsilon}}^{pl} \tag{7}$$

Where, C and γ are material constants from cyclic testing. C is for the kinematic shift of yield surface and γ is for the rate at which the saturation value of kinematic hardening decreases with increasing plastic strain. $\sigma_0 = \sigma_y + R$, where, σ_y is the yield stress for zero plastic strain. The back stress can be integrated from "Eq. (7)" for uniaxial case:

$$\alpha = \frac{C}{\gamma}(1 - e^{-\gamma\bar{\varepsilon}^{pl}}) + \alpha_1 e^{-\gamma\bar{\varepsilon}^{pl}} \tag{8}$$

Where, α_1 is came from the stabilized cycle and is given by $\alpha_1 = \sigma_1 - \sigma_s$, where α_1 is the stress at the start of the stabilized cycle and σ_s is the yield stress at the stabilized cycle.

$$\sigma s = \frac{\sigma_1 + \sigma_n}{2} \tag{9}$$

Where, σ_1 and σ_n are the stress at the start and end of the stabilized cycle.

3.3. Thermal Model

The thermomechanical plasticity theories have been proposed. The modified nonlinear isotropic hardening law is given by [12]:

$$R_{th} = Q\left(1 - e^{-b\underline{\varepsilon}^{pl}}\right) * (1 - \theta^m) \quad (10)$$

Where, m is the material parameter and θ is the nondimensional temperature given as:

$$\theta = \frac{\theta - \theta_{trans}}{\theta_{melt} - \theta_{trans}} \quad (11)$$

θ_{trans} transition is the transition temperature, at or below which there is no temperature dependence of yield stress, and θ_{melt} is the melting temperature. Similarly, the modified nonlinear kinematic hardening law is given by:

$$\alpha_{th} = \left(\frac{C}{\gamma}\left(1 - e^{-\gamma\bar{\varepsilon}^{pl}}\right) + \alpha_1 e^{-\gamma\bar{\varepsilon}^{pl}}\right) * (1 - \theta^m) \quad (12)$$

4 FE MODELING

To study the mechanical-thermal coupled behaviour of materials during ultrasonic welding, a 3D thermo-mechanically coupled model was developed with a general-purpose Abaqus software package. The developed model is able to investigate the effects of input parameters on temperature distribution, energy, and materials displacement during the process.

Figure 2 shows the 3D modelling configuration for the welding. Both horn and anvil had flat faces without any particular patterns. They were assumed as rigid bodies in the model. The aluminium foil is placed on top of the copper. The top and bottom foils were set as 20×20 mm with 0.2 mm thickness. The dimensions of the horn were set as 8×8 mm with 8 mm thickness while it was 9×9 mm with 9 mm thickness for the horn. An Abaqus 8-node brick element C3D8RT with a reduced integration scheme was applied for the foils, horn, and anvil, which has one degree of freedom for temperature and three degrees of freedom for deformation.

The number of work piece elements was 4842, while the horn and anvil were simultaneously modelled with 512 elements. The hourglass control mechanism was implemented in this study. The horn and anvil were considered as non-deformable rigid bodies, while the work piece materials were modelled as deformable. The contact conditions between components were defined by applying the Abaqus functionality "contact pair". For the sake of reducing the simulation time, the contact pair area between the foils was defined with the square area of 10 × 10 mm, which is shown in "Fig. 2(b)".

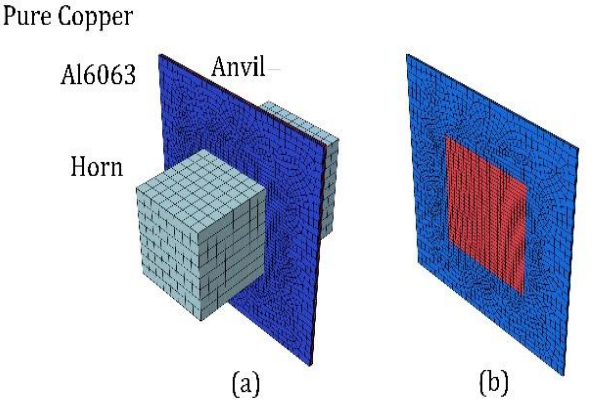

Fig. 2 (a): The geometry configuration with horn, anvil and the foils, and (b): the foils have a center square area (Red color) for defining contact in Abaqus.

To simulate the entire welding process in the software, the process should be divided into separate steps. These steps are shown in "Fig. 3". At the first step which is shown in "Fig.3(a)", clamping pressure is applied to the foils with the horn and anvil over a present time period. The clamping time is the time from the beginning of contact between the horn and top foil to the moment when the pressure attains its final amount. At this stage of modelling, there is only a mechanical part without any thermal term. Figure 3(b) shows the second step in modelling which involves the vibration of the horn and corresponding frictional heat generation. Since the heat factor is also introduced at this stage of the modelling, this step has modelled as a coupled thermal-mechanical case. The heat comes directly from slipping motion, clamping pressure and also frictional work by simulating the step as a dynamic thermal process.

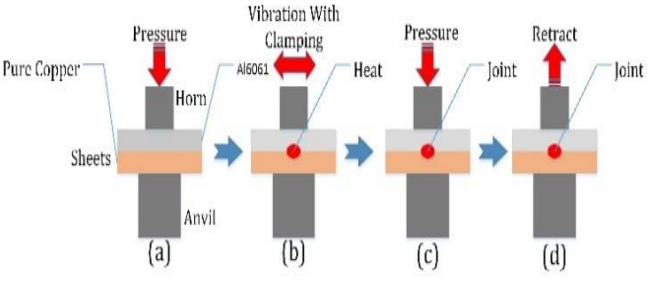

Fig. 3 Modeling configuration of ultrasonic welding. In the figure, a, b, c, d represents the order of executing simulation for each step.

At the next steps shown in "Fig. 3(c)" and "Fig.(d)", the weld forms, and then the horn returns and pressure is removed from the work pieces.

Figure 4 compares the simulation results of temperature with the experimental results obtained by Lee et. al [2]. The model simulations matched very well with the experimental results and hence the modelling of heat generation was verified.

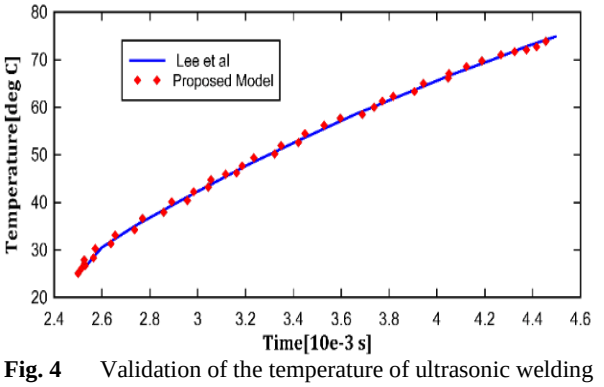

Fig. 4 Validation of the temperature of ultrasonic welding at a given time explored according to the default geometry.

The time-displacement diagram as a result of applying boundary conditions at the first 4.5 ms of simulations for 40 kHz frequency, 25μm amplitude and 100 MPa of clamping pressure is shown in "Fig. 5". Sinusoidal displacement was conducted to the horn which is defined as:

$$U(t) = u_0 . \sin(2\pi f . t) \quad (13)$$

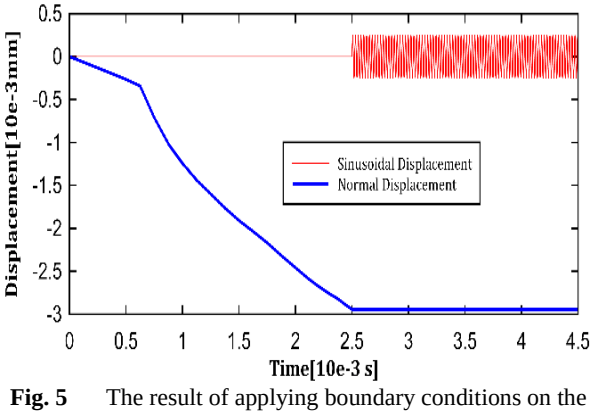

Fig. 5 The result of applying boundary conditions on the horn. Sinusoidal displacement (Red color), Normal direction displacement (Blue color).

5 RESULTS AND DISCUSSION

5.1. Effect of Clamping Pressure

As mentioned before, one of the important input parameters of the ultrasonic is the clamping force used in the process. In this section, to investigate the effect of clamping pressure on the weld properties, three different clamping pressure has been used in the modelling.

The simulation results in this section are shown in "Figs. 6 and 7". The results illustrated that when the clamping pressure increases, the weld area becomes wider. An increased weld area can increase the mechanical strength of the welded joint. The reason for increasing the weld area is seen in "Fig. 6". As seen in the temperature contours, the highest temperature appears in the model with the highest clamping force. The maximum temperature at the clamping force of 120 MPa is 338 °C. This value is 38°C greater than the maximum temperature of the model with the clamping pressure of 105 MPa. In a welding process, increasing the temperature of the weld area can increase the bonding surface of the two pieces. It has already been reported that increasing the clamping pressure increases the weld strength [3]. Moreover, it is noted that excessive pressure may produce high friction and hence limit the relative motion of the foils resulting in reduced weld strength. In addition, extensive deformation results in high clamping pressure needing a high power level by the system. Thus, a moderate clamping force is indispensable to generate intimate contact between the welded samples.

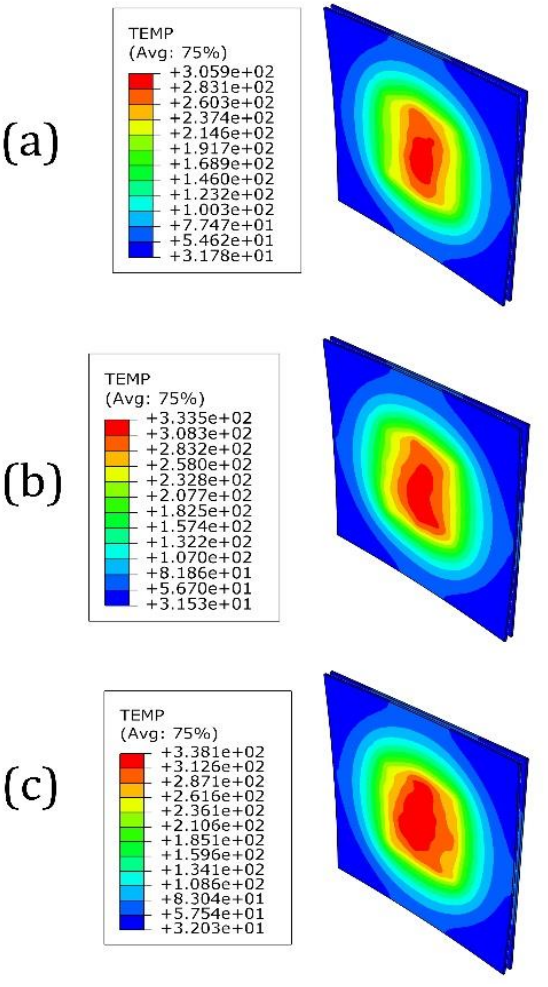

Fig. 6 Distribution of temperature: (a): 105 MPa, (b): 110 MPa, and (c): 120 MPa.

Figure 7 shows that at the beginning of the process for all of the chosen clamping forces, the temperature ignoring the acoustic softening effect grows more quickly. With the continuation of the process, the temperature growth rates decrease and come into saturation conditions. The conclusion is that the increase in temperature after a certain amount of time turns from a high to a low level which is consistent with the results of De Vries's work [4]. The difference in the temperatures obtained from modelling with different clamping pressures is also shown in "Fig. 7".

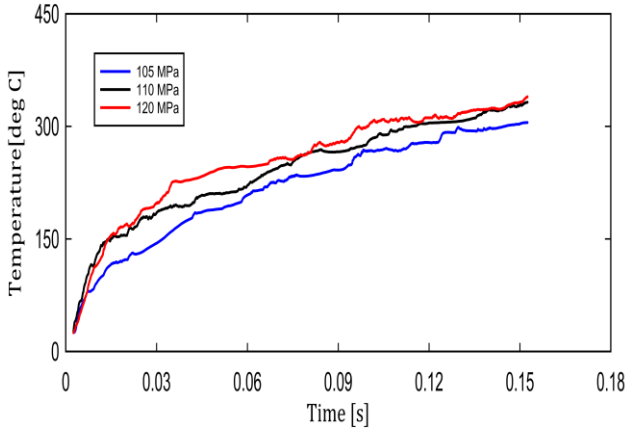

Fig. 7 Temperature histories of the center of aluminum foil.

5.2. Effect of Vibration Frequency

The properties of an ultrasonic welded joint are quite sensitive to the variation of process input parameters, such as clamping pressure and frequency. Inherently, the interactions among these parameters have a great effect on the quality of the welds. Previous research work has been observed, when the vibration frequency reaches 20 kHz, the high strain rates (103–105 s −1) can be achieved in a moment, due to the interface interaction between the welding materials [5].

In ultrasonic welding of aluminium sheets to copper, generally, frequencies ranging from 16 to 60 kHz are used [6-7]. At this present work, the ultrasonic welding process is analysed for 0.5 s at three different values of vibration frequency including 40, 50, and 60 kHz. Temperature predictions for different vibration frequencies are shown in "Fig. 8".

It can be seen from the figure that frequency has a significant impact on the temperature of the materials. The increase in temperature is due to the fact that the frequency is directly related to the amount of frictional heat production in terms of slipping velocity and distance. With the increasing frequency of vibration, the generated heat is also increased. The maximum temperature at a frequency of 60 kHz is about 200 degrees higher than the maximum temperature at a frequency of 40 kHz. It is also noticeable that the highest temperature rise occurred in the centre of the samples, an area located between the horn and anvil.

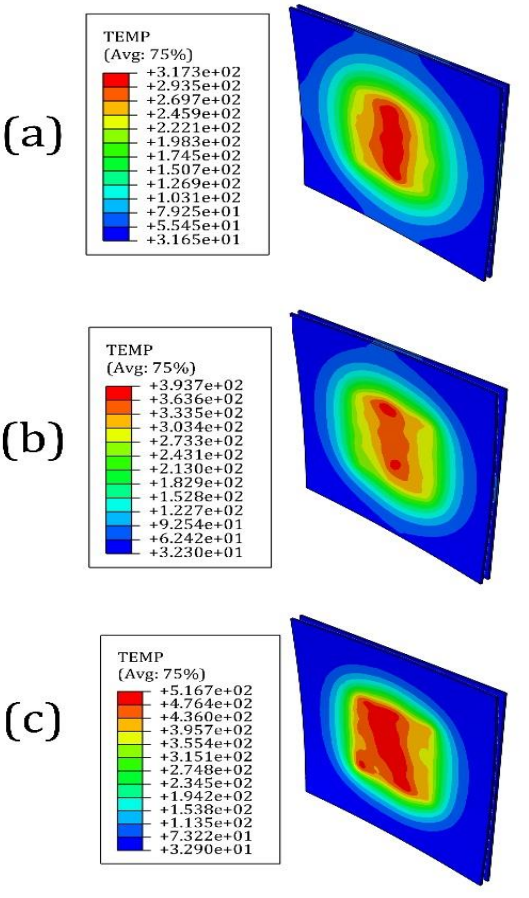

Fig. 8 Temperature distribution on the foils at different vibration frequencies: (a): 40 kHz, (b): 50 kHz, and (c): 60 kHz.

Although ultrasonic welding is a solid-state joining process that has lower peak temperature and temperature gradient, it is still a process accompanied by uneven heating and cooling in time and space. This localized uneven heating and cooling can cause plastic strain in the welded material during the process, and the resulting plastic strain cannot be fully recovered after welding. Accordingly, the residual deformation after ultrasonic welding is inevitable, and the unrecovered plastic strain is the source of residual deformation. Increasing the size of the work piece or reducing its thickness can lead to deformation after the welding process. Especially in large thin sheets, the residual deformation after ultrasonic welding cannot be ignored, which affects the dimensional accuracy and assembly quality.

Figure 9 shows the deformation of the foils in the thickness direction at three different vibration frequencies. The maximum deformation appeared at a frequency of 60 kHz, which is equal to 1.26 mm, while the deformation at the frequency of 40 kHz was 0.65 mm. It is clear that the deformation rate has increased

with increasing frequency. This is due to the fact that the rise in temperature of the materials reduces the energy required for deformation. This conclusion can be seen again in "Fig. 10", As can be seen in this figure, the temperature difference at different frequencies is significant.

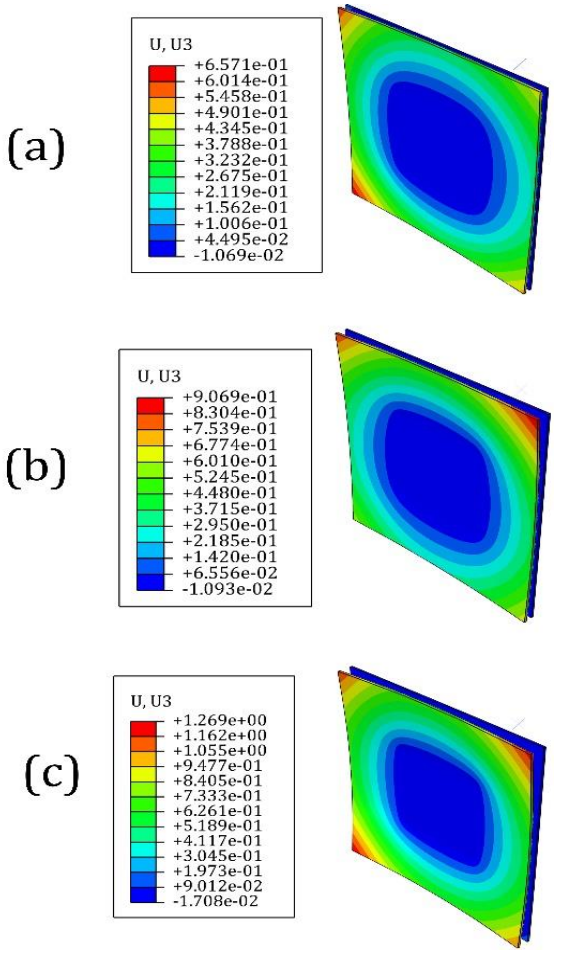

Fig. 9 Deformed shape of foils at different vibration frequencies: (a) 40 kHz, (b) 50 kHz, (c) 60 kHz.

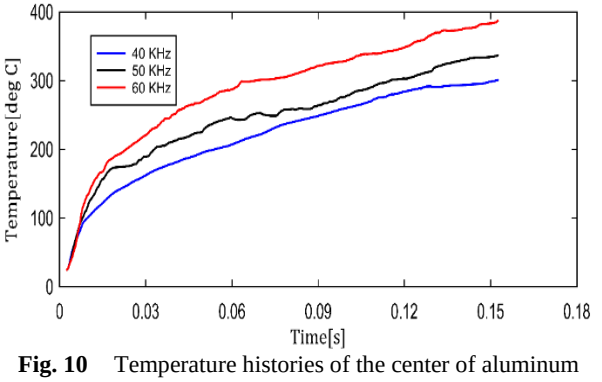

Fig. 10 Temperature histories of the center of aluminum foil.

5.3. Effect of Friction Coefficient

The friction behaviour is believed to be the most important behaviour of the ultrasonic welding process. It is well accepted that the characterization of the friction conditions at the foils interface is required for further understanding of the process. In ultrasonic welding, the friction affects the temperature of the bond region and the substrate. Variation of the coefficient of friction cause changes in the amount of heat generation during the ultrasonic welding process. Based on the simulation results, the ultrasonic vibration generates heat at the interface through friction; the heat lowers the mechanical properties of the material, which enhances localized plastic deformation in the sense that more plastic deformation generates more friction and heat. The effect of friction coefficient changes on the heat generated which is shown in the contours of "Fig. 11". When the coefficient of friction in the model is assumed to be 0.3, the maximum temperature has reached to 288 ˚C, while using the friction coefficient of 0.7 has reached to 317 ˚C.

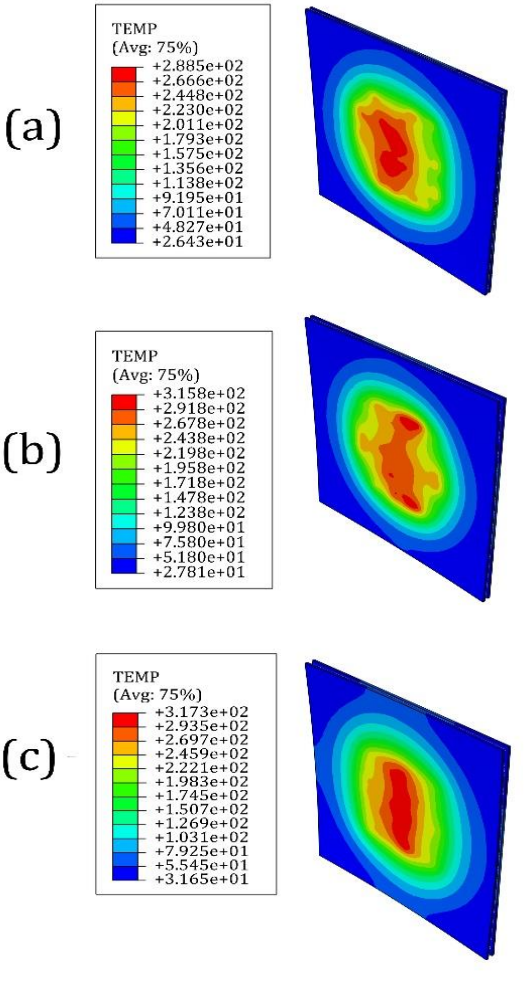

Fig. 11 Temperature distribution at different friction coefficients: (a): 0.3, (b): 0.5, and (c): 0.7.

6 CONCLUSIONS

Control of input parameters in ultrasonic welding through process modelling can guarantee that the required product properties are met with a minimum production cost. In this study, finite element theories were introduced and the simulation procedure using finite element analysis for ultrasonic welding of Al to Cu foils was established. The thermo-mechanically coupled analysis was conducted using (ABAQUS/EXPLICIT) finite element analyses and predicted the temperature distribution and foils distortion. The simulation results demonstrated that the clamping pressure, vibration frequency and friction coefficient have a great influence on heat production during the process which was critical to determine the final quality of the welded joint. The results of this study also showed that the proposed model is able to predict the effect of different welding parameters on the properties of the produced joint by studying temperature and deformation of the welded foils.

REFERENCES

[1] Ying Li, L. E., Flores, R. D., Elizabeth Trillo, A., and McClure, J. C., Intercalation Vortices and Related Microstructural Features in The Friction-Stir Welding of Dissimilar Metals, Materials Research Innovations, Vol. 2, No. 3, 1998, pp. 150–163. Doi: 10.1007/s100190050078.

[2] Watanabe, T., Sakuyama, H., and Yanagisawa, A., Ultrasonic Welding Between Mild Steel Sheet and Al–Mg Alloy Sheet, Journal of Materials Processing Technology, Vol. 209, No. 15–16, 2009 pp. 5475–5480. Doi: 10.1016/j.jmatprotec.2009.05.006.

[3] Shin, H. S., Leon De, M., Parametric Study in Similar Ultrasonic Spot Welding of A5052-H32 Alloy Sheets, J. Mater. Process. Technol., Vol. 224, 2015, pp. 222–232. Doi: 10.1016/j.jmatprotec.2015.05.013.

[4] Yang, J. W., Cao, B., He, X. C., and Luo, H. S., Microstructure Evolution and Mechanical Properties of Cu–Al Joints by Ultrasonic Welding, Science and Technology of Welding and Joining, Vol. 19, No. 6, 2014, pp. 500–504. Doi: 10.1179/1362171814Y.0000000218.

[5] Zhao, Y. Y., Li, D., and Zhang, Y. S., Effect of Welding Energy On Interface Zone of Al–Cu Ultrasonic Welded Joint, Science and Technology of Welding and Joining, Vol. 18, No. 4, 2013, pp. 354–360. Doi: 10.1179/1362171813Y.0000000114.

[6] Elangovan, S., Experimental and Theoretical Investigations On Temperature Distribution at The Joint Interface for Copper Joints Using Ultrasonic Welding, Manufacturing Review, Vol. 1, 2014, pp. 18. Doi: 10.1051/mfreview/2014017.

[7] Kim, T. H., Yum, J., Hu, S. J., Spicer, J. P., and Abell, J. A., Process Robustness of Single Lap Ultrasonic Welding of Thin, Dissimilar Materials, CIRP Annals, Vol. 60, No. 1, 2011, pp. 17–20, Doi: 10.1016/j.cirp.2011.03.016.

[8] Zhang, C. Y., Chen, D. L., and Luo, A. A., Joining 5754 Automotive Aluminium Alloy 2-mm-Thick Sheets Using Ultrasonic Spot Welding, Welding Journal, Vol. 93, 2014 pp. 131–138.

[9] De Vries, E., Mechanics and Mechanisms of Ultrasonic Metal Welding, Ph.D. Dissertation, The Ohio State University, pp. 253, 2004.

[10] Siddiq, A., Ghassemieh, E., Thermomechanical Analyses of Ultrasonic Welding Process Using Thermal and Acoustic Softening Effects, Mechanics of Materials, Vol. 40, No. 12, 2008, pp. 982–1000. Doi: 10.1016/j.mechmat.2008.06.004.

[11] Elangovan, S., Prakasan, K., and Jaiganesh, V., Optimization of Ultrasonic Welding Parameters for Copper to Copper Joints Using Design of Experiments, The International Journal of Advanced Manufacturing Technology, Vol. 51, No. 1–4, 2010, pp. 163–171. Doi: 10.1007/s00170-010-2627-1.

[12] Jedrasiak, P., Shercliff, H. R., Chen, Y. C., Wang, L., Prangnell, P., and Robson, J., Modelling of the Thermal Field in Dissimilar Alloy Ultrasonic Welding, Journal of Materials Engineering and Performance, Vol. 24, No. 2, 2014, pp. 799–807. Doi: 10.1007/s11665-014-1342-8.

[13] Elangovan, S., Semeer, S., and Prakasan, K., Temperature and Stress Distribution in Ultrasonic Metal Welding—An FEA-Based Study, Journal of Materials Processing Technology, Vol. 209, No. 3, 2009, pp. 1143–1150.

[14] Chen, K. K., Zhang, Y. S., Numerical Analysis of Temperature Distribution During Ultrasonic Welding Process for Dissimilar Automotive Alloys, Science and Technology of Welding and Joining, Vol. 20, No. 6, 2015, pp. 522–531. Doi: 10.1179/1362171815Y.0000000022.

[15] Konchakova, N., Balle, F., Barth, F. J., Mueller, R., Eifler, D., and Steinmann, P., Finite Element Analysis of an Inelastic Interface in Ultrasonic Welded Metal/Fibre-Reinforced Polymer Joints, Computational Materials Science, Vol. 50, No. 1, 2010, pp. 184–190. Doi: 10.1016/j.commatsci.2010.07.024.

[16] Lee, D., Kannatey-Asibu, E., and Cai, W., Ultrasonic Welding Simulations for Multiple Layers of Lithium-Ion Battery Tabs, Journal of Manufacturing Science and Engineering, Vol. 135, No. 6, 2013, pp. 061011. Doi: 10.1115/1.4025668.

[17] Zhang, C., Li, L., A Coupled Thermal-Mechanical Analysis of Ultrasonic Bonding Mechanism, Metallurgical and Materials Transactions, Vol. 40, No. 2, 2009, pp. 196–207, Doi: 10.1007/s11663-008-9224-9.

[18] Kim, T. H., Yum, J., Hu, S. J., Spice,r J. P., and Abell, J. A., Process Robustness of Single Lap Ultrasonic Welding of Thin, Dissimilar Materials, CIRP Annals - Manufacturing Technology, Vol. 60, No. 1, 2011, pp. 17–2. Doi: 10.1016/j.cirp.2011.03.016.

[19] Lee, D., Kannatey-Asibu, E., and Cai, W., Ultrasonic Welding Simulations for Multiple Layers of Lithium-Ion Battery Tabs, Journal of Manufacturing Science and Engineering, Vol. 135, No. 6, 2013, p. 061011. Doi: 10.1115/1.4025668.